

2-Dimensional Electrical Resistivity Tomography of Bitumen Occurrence in Agbabu, Southwestern, Nigeria.

ABSTRACT

The Electrical Resistivity Tomography (ERT) data was acquired within the area suspected to have high potential for bitumen occurrence using the Wenner-Schlumberger configuration. PASI 16GL-N Earth resistivity meter instrument was used to acquire data along five (5) traverses with 5m electrode spacing and traverses length 150m. The apparent resistivity values obtained were processed using RES2DINV software which helped to automatically obtain the 2D inversion model of the subsurface. This work has shown that the occurrence of bitumen was found between the depth of 13.4m and 9.93m for Traverses 1,2,3 and Traverses 4,5 respectively in 2-Dimensional electrical resistivity images which were corroborated by boreholes with a depth of about 18m. The results of this research indicated that the bitumen is characterized by good lateral continuity and is sufficiently thick for commercial exploitation (i.e. average thickness of 11.67m).

Keywords: Agbabu; Traverse; Bitumen; Occurrence; Depth

1. INTRODUCTION

The bedrock of Nigeria's economy before the discovery of petroleum deposits had been the solid minerals and agricultural sectors, but currently, it is the oil and gas sector. Over 80% of the country's revenue comes from export and domestic sales of oil and gas. As the hydrocarbon potentials of the prolific Niger Delta become depleted or in the near future may be exhausted due to continuous exploitation, attention needs to be shifted to other sources of revenue. Bitumen, which is known as asphalt or tar sand, is the heavy oil in the bituminous sand, which is a very dark coloured, sticky and highly viscous liquid or semi-solid form of petroleum. The occurrence and structural settings of the Agbabu tar sand (bitumen) deposits have been investigated due to the economic importance of bitumen as a readily available alternative source of energy [10].

Electrical resistivity tomography (ERT) is one of the most popular techniques for the shallow subsurface and is applied for hydrogeological, engineering, or agricultural questions. Applications cover a wide range of scales, from millimeter/centimeter scales at laboratory samples, decimeter to meter scale in soils, meter to decimeters for groundwater questions, but can reach several hundred meters or even kilometers for deep geological structures.

Variations in electrical resistivity (or conductivity) typically correlate with variations in lithology, water saturation, fluid conductivity, porosity and permeability, which may be used to map stratigraphic units, geological structure, sinkholes, fractures and groundwater. Resistivity data are then recorded via complex combinations of current and potential electrode pairs to build up a pseudo cross-section of apparent resistivity beneath the survey line. The depth of

38 investigation depends on the electrode separation and geometry, with greater electrode
39 separations yielding bulk resistivity measurements from greater depths.

40 The recorded data are transferred to a PC for processing. In order to derive a cross-sectional
41 model of true ground resistivity, the measured data are subject to a finite-difference inversion
42 process using the RES2DINV software.

43 Data processing is based on an iterative routine involving determination of a two-dimensional
44 (2D) simulated model of the subsurface. Convergence between theoretical and observed data is
45 achieved by non-linear least squares optimization. The extent to which the observed and
46 calculated theoretical models agree is an indication of the validity of the true resistivity model
47 (indicated by the final root-mean-squared (RMS) error).

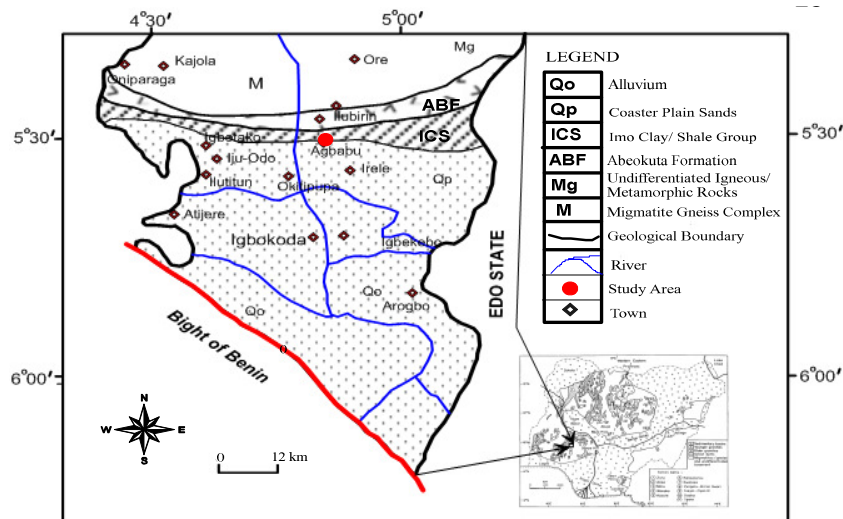
48 The true resistivity models are presented as colour contour sections revealing spatial variation in
49 subsurface resistivity. The 2D method of presenting resistivity data is limited where highly irregular
50 or complex geological features are present. Constraints: Readings can be affected by poor electrical
51 contact at the surface. An increased electrode array length is required to locate increased depths of
52 interest therefore the site layout must permit long arrays. Resolution of target features decreases
53 with increased depth of burial. To interpret the data from a 2-D imaging survey, a 2-D model for the
54 sub-surface which consists of a large number of rectangular blocks is usually use. A computer
55 program is then use to determine the resistivity of the blocks so that the calculated apparent
56 resistivity values agree with the measured values from the field survey [8]. The computer program
57 RES2DINV will automatically subdivide the subsurface into a number of blocks, and it then uses a
58 least-square inversion scheme to determine the appropriate resistivity value for each block. The
59 location of the electrodes and apparent resistivity values must be entered into a number of blocks,
60 and it then uses a least-squares inversion scheme to determine the appropriate resistivity value for
61 each block. apparent resistivity values must be entered into text file which can be read by the
62 RES2DINV program [9].

63 **1.1 Geology and description of the study area**

64 The study area is located within the geographical grids of latitude 6° 35' 16.3" N and 6° 37' 13.9"
65 N and longitude 4° 49' 29.0" E and 4° 50' 20.7" E in Odigbo local government area of Ondo
66 State. It falls within the sedimentary terrain in the Dahomey basin of southwestern, Nigeria.

67 The Dahomey basin is an Atlantic margin basin containing Mesozoic-Cenozoic sedimentary
68 succession reaching a thickness of over 3000m. It extends from south-eastern Ghana to the
69 western flank of the Niger Delta. It stratigraphy is classified by various authors into Abeokuta
70 Group, Imo Group, Oshosun Formation, Ilaro Formation and Coastal Plain sands and Alluvium
71 [1, 2, 6]. The Agbabu area is underlain by the sediments of the Imo group.

72



83
 84 **Figure 1:** Geological Map of southern part of Ondo State showing the Study Area
 85 (Modified After PTF, 1997).
 86

87 **2. METHODOLOGY**

88 In this research work, the wenner- schlumberger array in electrical resistivity survey was
 89 adopted. The investigation was carried out in Agbabu, southwestern, Ondo state, Nigeria. The
 90 basic field equipment for this study is the PASI 16 GL-N Earth resistivity meter.
 91 This is a new hybrid between the Wenner-Schlumberger arrays arising out of the relatively
 92 recent work with electrical imaging surveys [10]. The classical Schlumberger array is one of the
 93 most commonly used array for resistivity sounding survey. The “n” factor for this array is the
 94 ratio of the distance between the $C_1—P_1$ (or $P_2—C_2$) electrodes to the spacing between the
 95 $P_1—P_2$ potential pair. The sensitivity pattern for the schlumberger array is slightly different from
 96 the Wenner array with a slight vertical curvature below the center of the array, slightly lower
 97 sensitivity values in the regions between the C_1 and P_1 (P_2 and C_2) also and electrodes. There is a
 98 slightly greater concentration of high sensitivity values below the $P_1—P_2$ electrodes. This means
 99 that this array is moderately sensitive to both horizontal and vertical structures. In areas where
 100 both of geological structures are expected this array might be a good compromise between the
 101 Wenner and the dipole-dipole-array. The median depth of investigation for this array is about
 102 10% larger than that for the Wenner array for the same distance between the outer
 103 (C_1 and C_2) electrodes. The signal strength for this array is smaller than that for the Wenner array,
 104 but it is higher than the dipole-dipole array [8].

105
 106
 107
 108
 109

110
 111
 112
 113
 114
 115
 116
 117
 118
 119
 120
 121
 122
 123
 124
 125
 126
 127
 128
 129
 130
 131
 132
 133

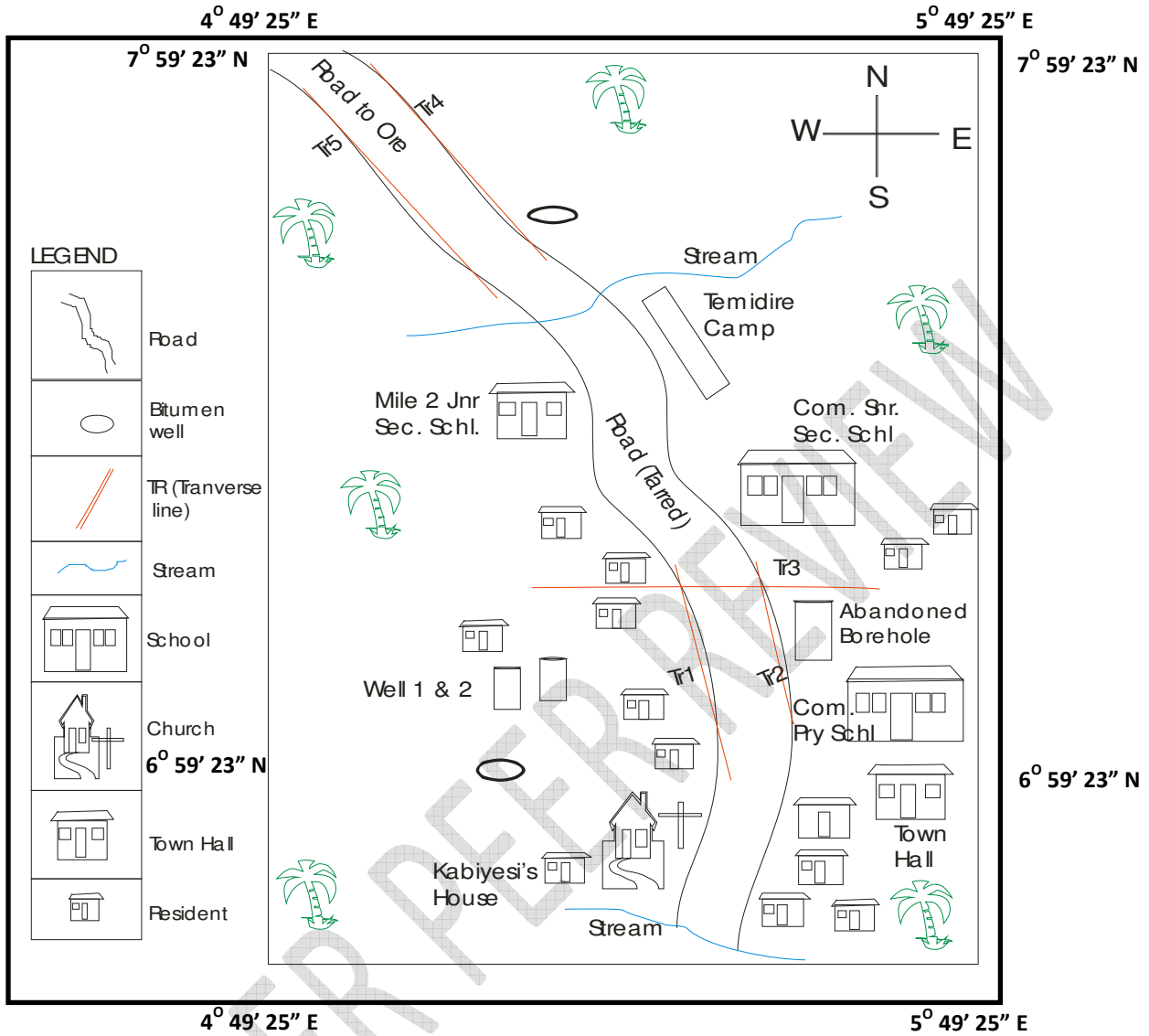


Figure 2: Base Map of the Study Area

2.1 Theory of electrical resistivity method for wenner-schlumberger array

From the theory, we have that the potential at M due to A is

$$V_M = \frac{\rho I}{2\pi} \left[\frac{1}{a(n+1)} - \frac{1}{na} \right]$$

Where a = midpoint = electrode spacing

n = integer value , ρ = layer resistivity

The potential at N due to B is

$$V_N = \frac{\rho I}{2\pi} \left[\frac{1}{a(n+1)} - \frac{1}{na} \right]$$

134 The potential difference dV between the two potential is therefore given by

$$\begin{aligned}
 135 \quad dV &= V_M - V_N \\
 136 \quad &= \frac{\rho I}{2\pi} \left[\left(\frac{1}{a(n+1)} - \frac{1}{na} \right) - \left(\frac{1}{a(n+1)} - \frac{1}{na} \right) \right] \\
 137 \quad &= \frac{\rho I}{2\pi} \left[\left(\frac{1}{a(n+1)} - \frac{1}{na} \right) - \frac{1}{a(n+1)} + \frac{1}{na} \right] \\
 138 \quad &= \frac{\rho I}{2\pi} \left[\left(\frac{1}{a(n+1)} - \frac{1}{na} \right) - \frac{1}{a(n+1)} + \frac{1}{na} \right] \\
 139 \quad &= \frac{\rho I}{2\pi} \left(\frac{(n+1) - n - n + (n+1)}{an(n+1)} \right) \\
 140 \quad dV &= \frac{\rho I}{2\pi} \left(\frac{2(n+1) - 2n}{an(n+1)} \right) = \frac{\rho I}{2\pi} \left(\frac{2}{an(n+1)} \right)
 \end{aligned}$$

141 Therefore, $\rho = \frac{dV\pi}{I} [an(n+1)]$.

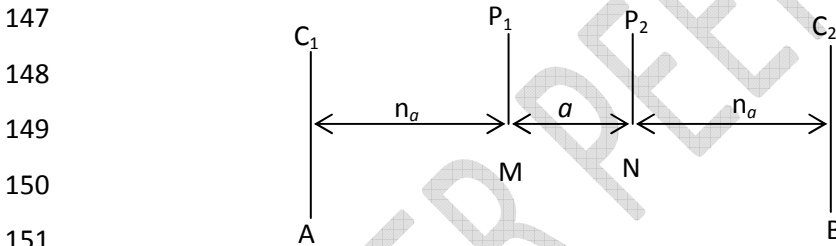
142 Where $\frac{dV}{I} = R\rho = R\pi [an(n+1)]$

143 $k = \pi [an(n+1)]$

144 Then, $\rho = RK$

145 Where k is the geometric factor.

146



153 **Figure 3:** Sketch of Wenner- Schlumberger array

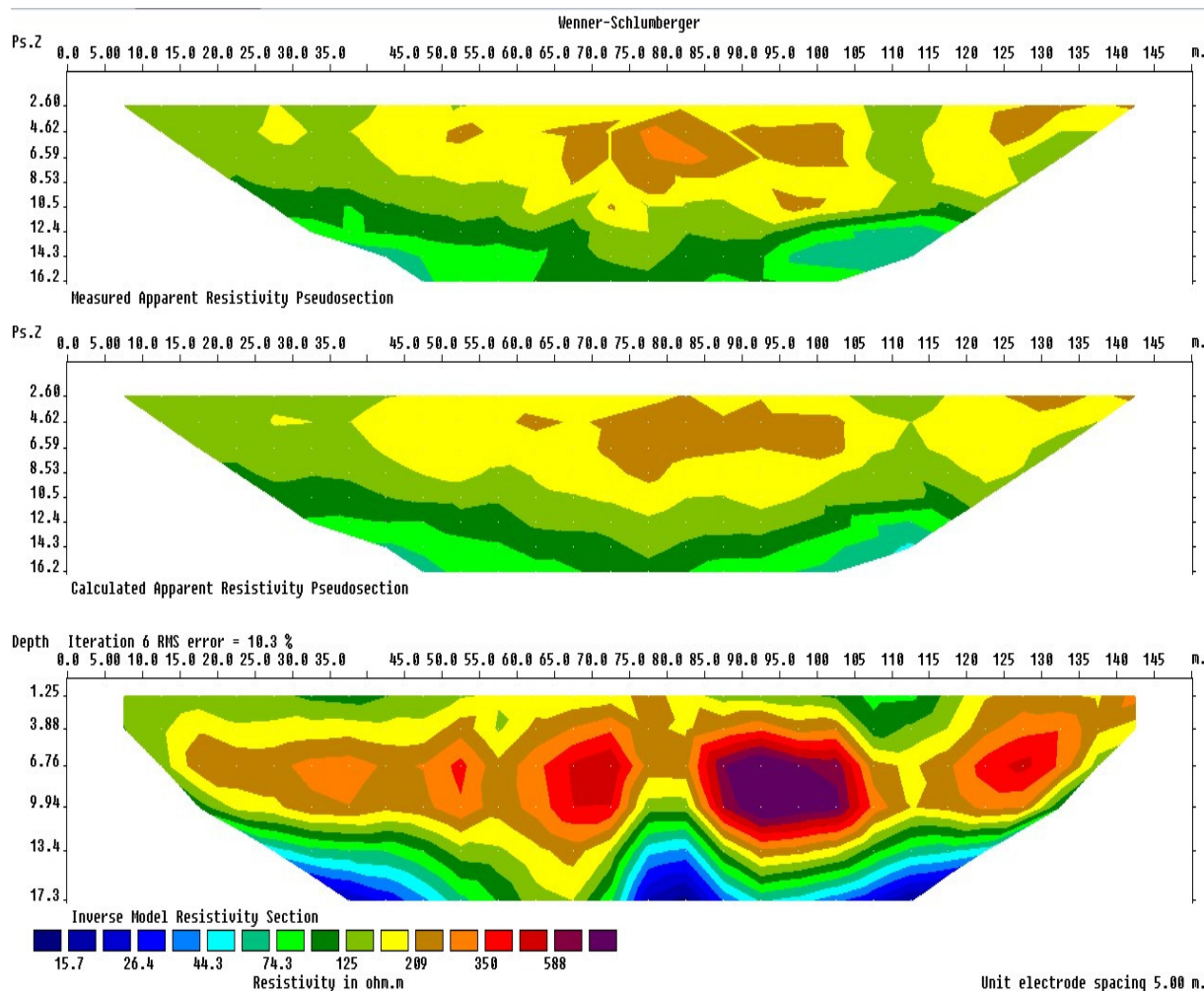
154

155 3. RESULTS AND DISCUSSION

156 **Agbabu Traverse One:** The inverted 2-D resistivity section shows the image of the subsurface
 157 to a depth of 17.3m as shown in Figure 4. The length of this traverse is 150m and oriented in an
 158 approximately N – S direction. The first layer designated with green and yellow colour has
 159 resistivity values in the range of 75 - 210Ωm. It can be seen from this profile that the topsoil
 160 which varies between 0- 3.88m in depth with thickness of 3.88m could probably consist of sandy
 161 soil.

162 The second geo-electric layer has resistivity in the range of 200 - 700Ωm which is indicated by
 163 brown, deep brown, red and purple. This formation occurs at a depth of 3.88m – 13.4m between
 164 lateral distances 52m -53m, 63m-72m, 84m-107m and 121m-132m could possibly be

165 accumulated of bitumen. Evidently, the profile length of 84m- 107m has a sharp increase of
 166 resistivity (500 - 700Ωm) which could now indicate possible accumulation of bitumen. The third
 167 layer has a low resistivity from 10 – 74.3Ωm. It has a thickness of about 3.9m and could be a
 168 possible aquiferous zone.



169

170

171 **Figure 4:** Inverted 2D-Resistivity Section along Traverse one

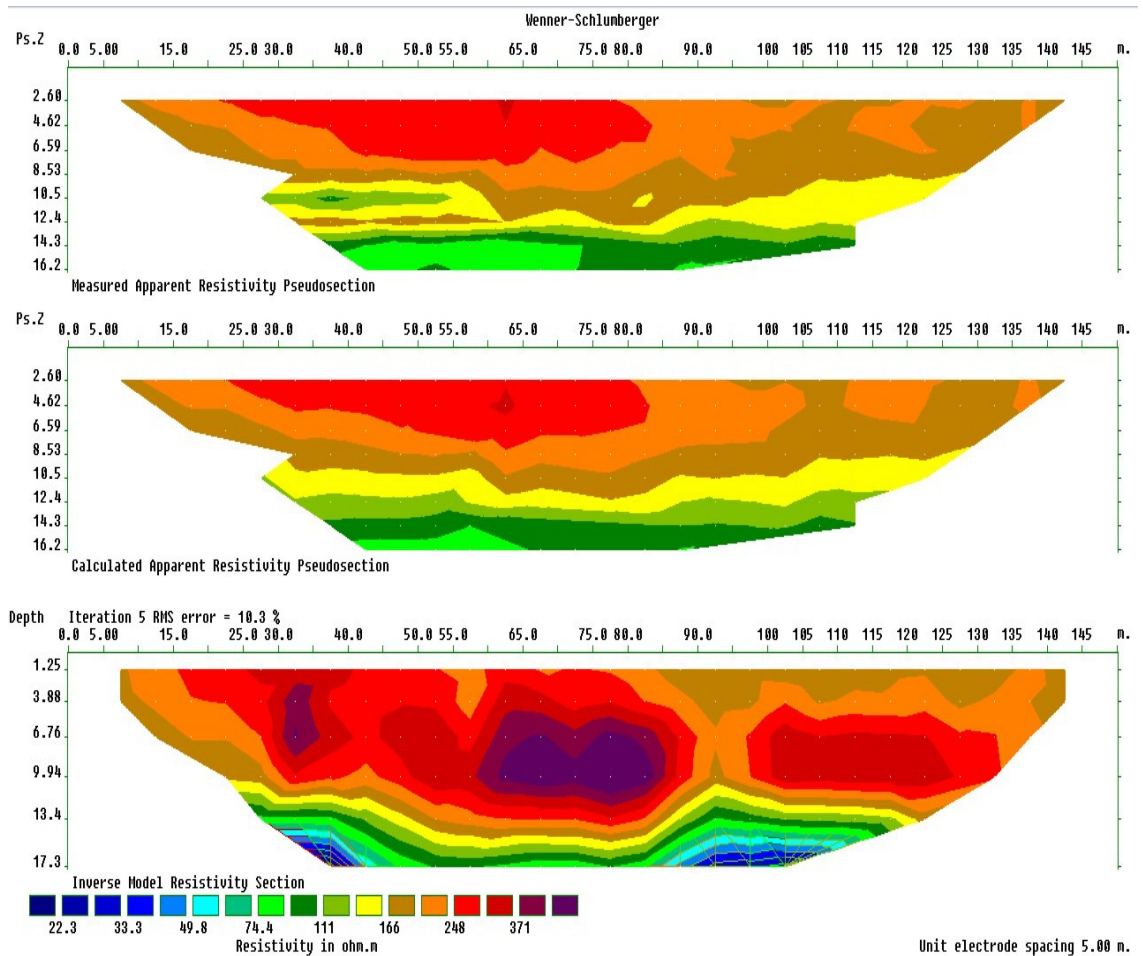
172 **Agbabu Traverse Two:** The inverted 2-D resistivity section shows the image of the subsurface
 173 to a depth of 17.3m as shown in Figure 5. The length of this traverse is 150m and oriented in an
 174 approximately N–S direction. The first layer has an increase resistivity values ranging from 166 -
 175 495Ωm designated with brown, deep brown, red and purple. This formation occurs at a depth of
 176 0 – 13.4m between lateral distances 30m -40m, 60m-85m and 98m-132m could possibly be
 177 accumulated of bitumen. Evidently, the profile length of 30m -40m and 60m-85m having a
 178 sharp increase of resistivity (371 - 495Ωm) which could now indicate possible accumulation of
 179 bitumen.

180 The second geo-electric layer has undulating thickness between 2.15 and 3.9m down the profile
 181 with resistivity values between 74.4- 166Ωm could probably consist of sandy soil. The third

182 geo-electric layer extends to a depth from 15.3m-17.3m along a lateral distances 30m-40m and
 183 85m-110m has a low resistivity from 10 – 50Ωm. It has a thickness of about 2m could possibly
 184 serve as a perched aquifer.

185

186



187

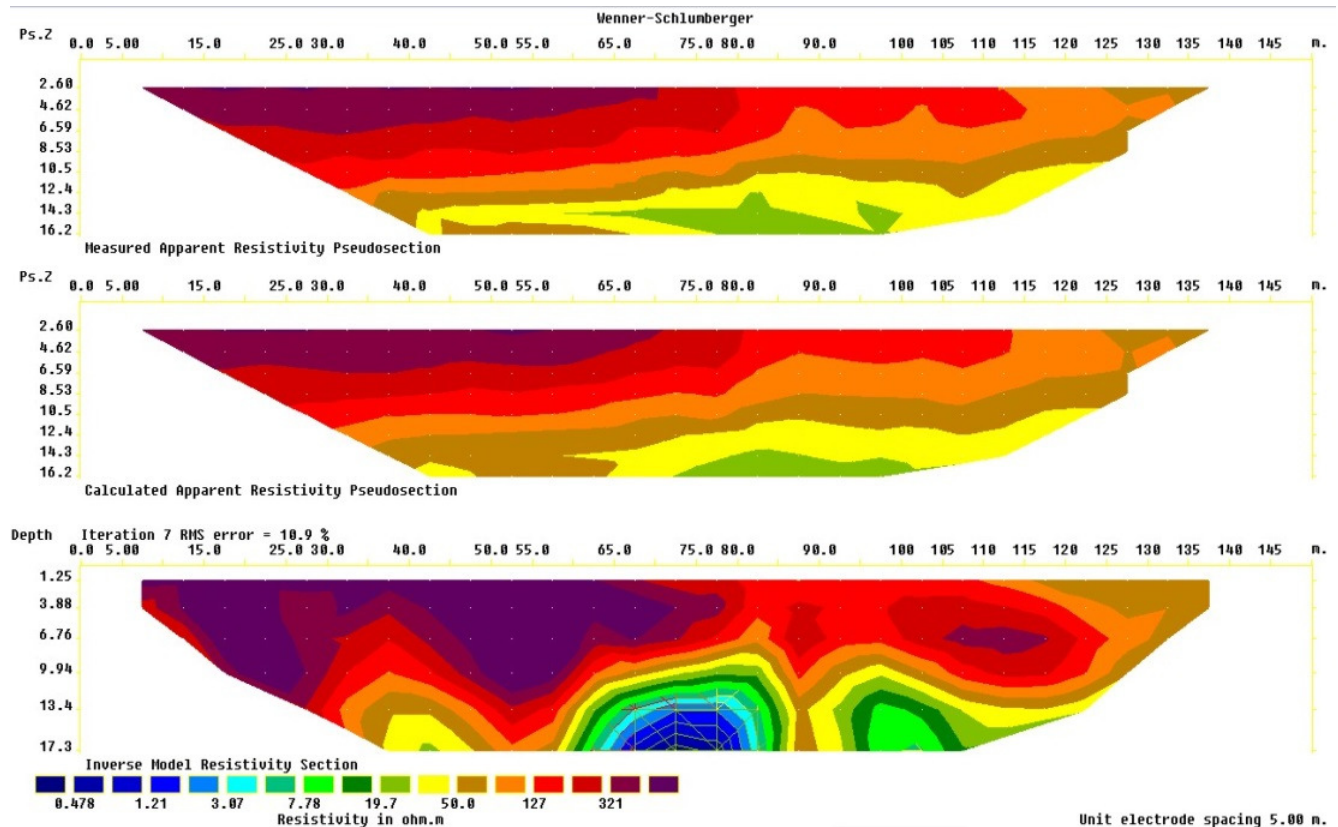
188

Figure 5: Inverted 2D-Resistivity Section along Traverse Two

189 **Agbabu Traverse Three:** The inverted 2-D resistivity section shows the image of the
 190 subsurface to a depth of 17.3m as shown in Figure 6. The length of this traverse is 150m and
 191 oriented in an approximately W–E direction. The first layer has an increase resistivity values
 192 ranging from 127 - 515Ωm designated with red and purple. This formation occurs at a depth of 0
 193 – 13.4m between lateral distances 8m-125m could possibly be accumulated of bitumen.
 194 Evidently, the profile length of 8m -77m and 105m-117m having a sharp increase of
 195 resistivity(321 - 515Ωm) which could now indicate possible accumulation of bitumen.

196 The second geo-electric layer designated with brown yellow and green colour has undulating
 197 depth varies from 1.25 - 17.3m down the profile with resistivity values between 7.78- 127Ωm
 198 could indicate the presence of sandy soil of varying porosity and permeability. The third geo-
 199 electric layer designated with light blue and deep blue colour extends to a depth from 13.4m-

200 17.3m along a lateral distances 65m-80m having a low resistivity from 0 – 7.78Ωm. It has a
 201 thickness of about 3.9m which could possibly serve as a perched aquifer.
 202 The three traverses show similar features at depth 13.4m. This correlation could indicate the
 203 presence of possible accumulation of bitumen at this depth.
 204



205
 206 **Figure 6:** Inverted 2D-Resistivity Section along Traverse Three

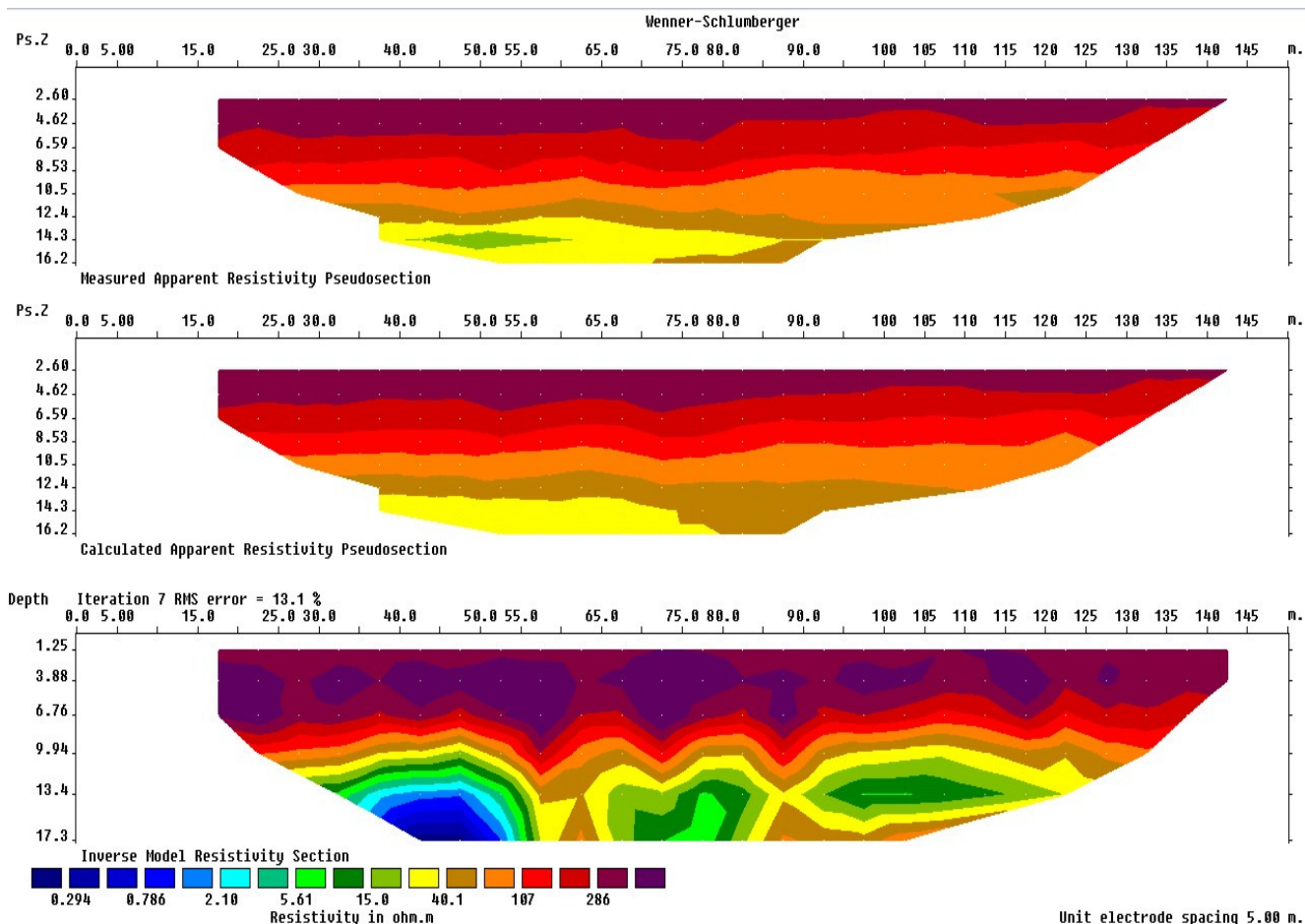
207 **Agbabu Traverse Four:** The inverted 2-D resistivity section shows the image of the subsurface
 208 to a depth of 17.3m as shown in Figure 7. The length of this traverse is 150m and oriented in an
 209 approximately N–S direction.

210 The first layer has an increase resistivity values ranging from 107 - 465Ωm designated with red
 211 and purple colour. This formation occurs at a depth of 9.94m along a lateral distances 17.5m-
 212 142.5m could possibly be accumulated of bitumen. It has a thickness ranging from 1.25m-9.94m.
 213 Evidently, the lateral profile length having a sharp increase of resistivity (286 - 465Ωm) could
 214 now indicate possible accumulation of bitumen.

215 The second geo-electric layer designated with brown, yellow and green colour has undulating
 216 along lateral distance 35m-55m. It has resistivity values between 5.61- 107Ωm could probably
 217 consist of sandy soil. This formation has a thickness varying from 9.94m-17.3m. The third geo-

218 electric layer designated with light blue and deep blue colour extends to a depth from 13.34m-
 219 17.3m along a lateral distances 34m-53m having a low resistivity from 0 – 5.61Ωm. It has a
 220 thickness of about 3.9m which could possibly host a large volume of underground water
 221 resources.

222



223

224

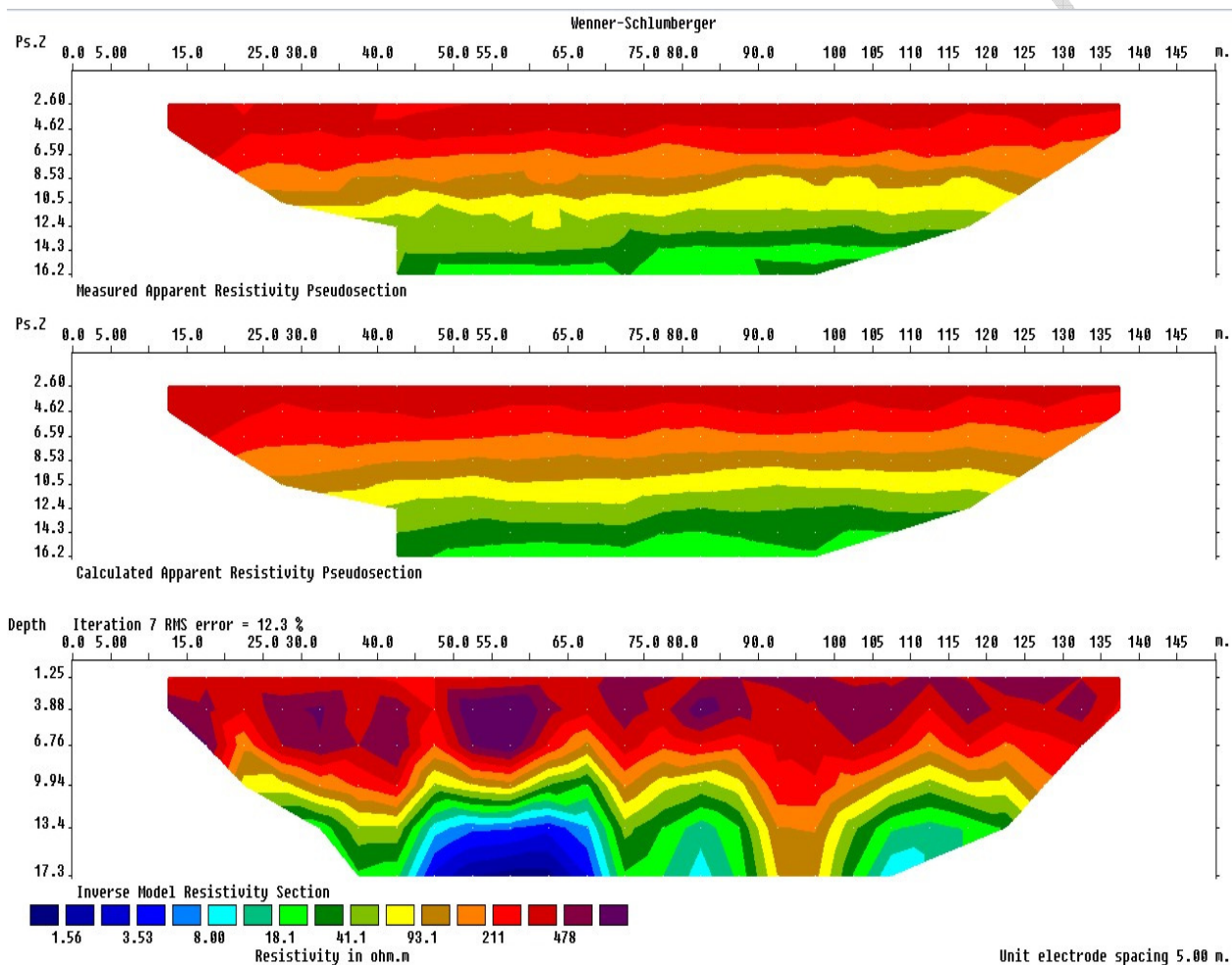
Figure 7: Inverted 2D-Resistivity Section along Traverse Four

225 **Agbabu Traverse Five:** The inverted 2-D resistivity section shows the image of the subsurface
 226 to a depth of 17.3m as shown in Figure 8. The length of this traverse is 150m and oriented in an
 227 approximately N - S direction.

228 The first layer has an increase resistivity values ranging from 211 - 745Ωm designated with red
 229 and purple colour. This formation occurs at a depth of 9.94m along a lateral distances 12.5m-
 230 137.5m could possibly be accumulated of bitumen. It has a thickness ranging from 0-9.94m.
 231 Evidently, the lateral profile length having a sharp increase of resistivity (478 - 745Ωm) could
 232 now indicate possible accumulation of bitumen.

233 The second geo-electric layer designated with brown, yellow and green colour has undulating
 234 along lateral distance 47m-67m, 78m-62m and 105m 115m. It has resistivity values between

235 18.1- 211Ωm could probably consist of sandy soil. This formation has a thickness varying from
 236 8.35m-17.3m. The third geo-electric layer designated with light blue and deep blue colour
 237 extends to a depth from13.4m-17.3m along a lateral distances 34m-53m having a low resistivity
 238 from 1m – 8.2Ωm. It has a thickness of about 3.9m which could possibly host a large volume of
 239 underground water resources.
 240 Traverse 4 and 5 having correlation of the same depth of 13.4m that could possibly be
 241 accumulated of bitumen.
 242

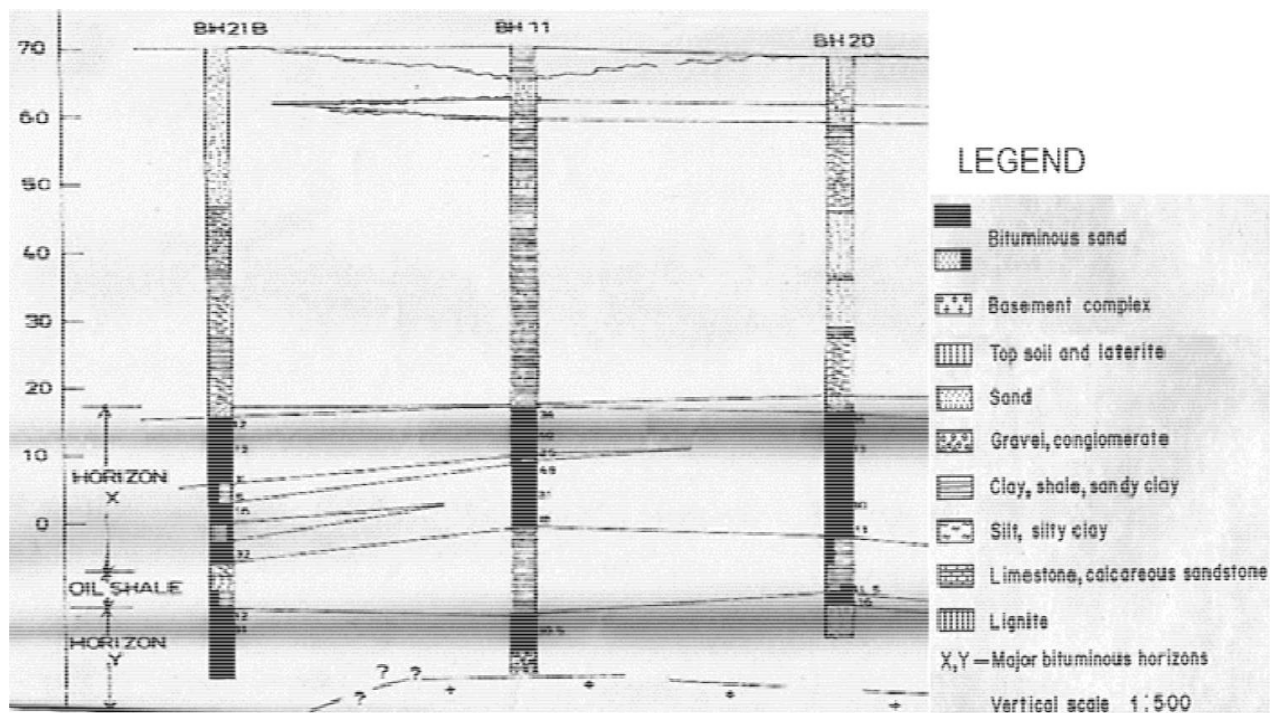


243

244

Figure 8: Inverted 2D-Resistivity Section along Traverse Five

245



246

247

Figure 9:Lithofacies / Bitumen Saturation Correlation Panel of the Study Area

248

(Modified after GCU, Uni. of Ile-Ife, 1980) [4].

249

250 5. CONCLUSION

251 This research has shown that the occurrence of bitumen was found between the depth of 13.4m
 252 and 9.93m for Traverses 1,2,3 and Traverses 4,5 respectively corroborated by boreholes with a
 253 depth of about 18m. The results of this research indicated that the bitumen is characterized by
 254 good lateral continuity and sufficiently thick for commercial exploitation (i.e. average thickness
 255 of 11.67 m). Bitumen and tar bearing sands formation are known to be characterized by high
 256 resistivity [3]. Low resistivity values are encountered in places where the bitumen is thought to
 257 be associated with saline water [5].

258

259 REFERENCES

- 260 1. Adegoke, O.S., and Omatsola, M.E., (1981). "Tectonic Evolution and Cretaceous
 261 Stratigraphy of the Dahomey Basin". J. Min. Geol. 18 (1): 130-137.
 262 2. Agagu, O.K., (1985). A geological guide to Bituminous Sediments in South-Western
 263 Nigeria: Unpublished Report, Department of Geology, University of Ibadan.
 264 3. Eke, E., (2005). Geoelectric Delineation of near-surface Tar sand Deposit in Agbabu,
 265 Ondo State, Southwestern Nigeria Unpublished M. Tech; Thesis, Federal University of
 266 Technology, Akure. 88pp.
 267 4. Geological Consultancy Unit, University of Ile – Ife (1980). Geotechnical Investigation

- 268 of the Ondo State Bituminous Sands. Vol. 1, Folio 15. Unpublished Gwynn, J. W, and
269 Hanson, F. V., 2009. Annotated Bibliography of Utah Tar Sand Deposits, Open-file
270 Report 503Utah Geological Survey p. 1 – 4.
- 271 5. Halliburton, A.D., (2001). Basic Petroleum Geology and Analysis. Halliburton Company,
272 SOP.
- 273 6. Jones, H.A., and Hockey, R.D., (1964). “The Geology of Part of South-western Nigeria”.
274 Geol. Surv. Nigeria Bull. 31: 87.
- 275 7. Loke, M.H., (2004): Tutorial 2D and 3D Electrical Imaging Surveys. Available at
276 www.geoelectrical.com, 28pp.
- 277 8. Loke, M.H., and Barker, R.D., (1995). Least-Squares Deconvolution of Apparent
278 Resistivity Pseudosections. Geophysics, 60, p 1682-1690.
- 279 9. Obiora, D.N., Ossai, M.N., Okwoli,E., (2015). A case study of aeromagnetic data
280 interpretation. International Journal of Physical Sciences 10(17), 503-519.
- 281 10. Pazdirek, O. and Blaha, V., (1996). Examples of resistivity imaging using ME-100
282 resistivity field acquisition system. EAGE 58th Conference and TechnicalExhibition
283 Extended Abstracts, Amsterdam.

284

285

286

287

288